



1 **Gas transfer velocities of CO₂ in subtropical monsoonal climate streams and**
2 **small rivers**

3

4 **Siyue Li^{a*}, Rong Mao^a, Yongmei Ma^a, Vedula V. S. S. Sarma^b**

5 a. Chongqing Institute of Green and Intelligent Technology, Chinese Academy of
6 Sciences, Chongqing 400714, China

7 b. CSIR-National Institute of Oceanography, Regional Centre, Visakhapatnam, India

8

9 **Correspondence**

10 **Siyue Li**

11 *Chongqing Institute of Green and Intelligent Technology (CIGIT),*

12 *Chinese Academy of Sciences (CAS).*

13 *266, Fangzheng Avenue, Shuitu High-tech Park, Beibei, Chongqing 400714, China.*

14 *Tel: +86 23 65935058; Fax: +86 23 65935000*

15 *Email: syli2006@163.com*



16 **Abstract**

17 CO₂ outgassing from rivers is a critical component for evaluating riverine carbon
18 cycle, but it is poorly quantified largely due to limited measurements and modeling of
19 gas transfer velocity (*k*) in subtropical streams and rivers. We measured CO₂ flux
20 rates, *k* and partial pressure (*p*CO₂) in river networks of the Three Gorges Reservoir
21 (TGR) region, a typical area in the upper Yangtze River with monsoonal climate and
22 mountainous terrain. The observed *k* values ($k_{600}=48.4\pm 53.2$ cm/h) were showed large
23 variability due to spatial variations in physical controls on surface water turbulence.
24 Our *k* measurements using chambers were comparable with model derived velocities.
25 Unlike in open waters, *k* is more pertinent to flow velocity and water depth in the
26 studied small rivers. Our results show that TGR river networks emitted approx. 1.4 Tg
27 CO₂/y using varying approaches such as chambers, measured *k* and developed *k*
28 model. This study suggests that incorporating scale-appropriate *k* measurements into
29 extensive *p*CO₂ investigation is required to refine basin-wide carbon budgets in the
30 subtropical streams and small rivers. We concluded that simple parameterization of *k*
31 as a function of morphological characteristics was site specific and hence highly
32 variable. *k* models should be developed for stream studies to evaluate the contribution
33 of these regions to atmospheric CO₂.

34

35 **Key words:** CO₂ outgassing, riverine C flux, flow velocity, physical controls, Three

36 Gorge Reservoir, Yangtze River



37 1. Introduction

38 Rivers serve as a significant contributor of CO₂ to the atmosphere (Cole *et al.*,
39 2007; Tranvik *et al.*, 2009; Li *et al.*, 2012; Raymond *et al.*, 2013). As a consequence,
40 accurate quantification of riverine CO₂ emissions is a key component to estimate net
41 continental carbon (C) flux (Bastviken *et al.*, 2011). More detailed observational data
42 and new accurate measurement techniques are critical to refine the riverine C budgets
43 (Raymond and Cole, 2001; Li and Bush, 2015). Generally two methods are used to
44 estimate CO₂ areal fluxes from the river system, such as direct measurements floating
45 chambers (FCs), and indirect calculation of thin boundary layer (TBL) model that
46 depends on gas concentration at air-water gradient and gas transfer velocity, k (Guerin
47 *et al.*, 2007; Xiao *et al.*, 2014). Direct measurements are normally laborious, while the
48 latter method shows ease and simplicity and thus is preferred (Butman and Raymond,
49 2011; Li *et al.*, 2012; Li *et al.*, 2013; Lauerwald *et al.*, 2015; Ran *et al.*, 2015).

50 The areal flux of CO₂ (F , unit in mmol/m²/d) *via* the water–air interface by TBL
51 is described as follows:

$$52 F = k \times K_h \times \Delta pCO_2 \quad (1)$$

$$53 K_h = 10^{-(1.11 + 0.016 * T - 0.00007 * T^2)} \quad (2)$$

54 where k (unit in m/d) is the gas transfer velocity of CO₂ (also referred to as piston
55 velocity) at the *in situ* temperature (Li *et al.*, 2016). ΔpCO_2 (unit in μatm) is the
56 air-water gradient of pCO_2 (Borges *et al.*, 2004a). K_h (mmol/m³/ μatm) is the
57 aqueous-phase solubility coefficient of CO₂ corrected using temperature (T in $^{\circ}\text{C}$) (Li
58 *et al.*, 2016).



59 $\Delta p\text{CO}_2$ can be measured precisely in various aquatic systems, however, the
60 accuracy of the estimation of flux is depended on the k value. Broad ranges of k for
61 CO_2 (Raymond and Cole, 2001; Borges *et al.*, 2004a; Raymond *et al.*, 2012) were
62 reported due to variations in techniques, tracers used and governing processes. k is
63 controlled by turbulence at the surface aqueous boundary layer, hence, k_{600} is
64 parameterized as a function of wind speed in open water systems of reservoirs, lakes,
65 and oceans (Borges *et al.*, 2004b; Guerin *et al.*, 2007; Wanninkhof *et al.*, 2009). While
66 in streams and small rivers, turbulence at the water-air interface is generated by shear
67 stresses at streambed, thus k is modeled using channel slope, water depth, and water
68 velocity in particular (Alin *et al.*, 2011; Raymond *et al.*, 2012). Variable formulations
69 of k have been established by numerous theoretical, laboratory and field studies,
70 nonetheless, better constraint on k levels is still required as its levels are very
71 significant and specific due to large heterogeneity in hydrodynamics and physical
72 characteristics of river networks. This highlights the importance of k measurements in
73 a wide range of environments for the accurate upscaling of CO_2 evasion, and for
74 parameterizing the physical controls on k_{600} . However, only few studies provide
75 information of k for riverine CO_2 flux in Asia (Alin *et al.*, 2011; Ran *et al.*, 2015), and
76 those studies do not address the variability of k in China's small rivers and streams.

77 Limited studies demonstrated that higher levels of k in the Chinese large rivers
78 (Alin *et al.*, 2011; Ran *et al.*, 2015; Liu *et al.*, 2017; Ran *et al.*, 2017), which
79 contributed to much higher CO_2 areal flux particularly in China's monsoonal rivers
80 that are impacted by concentrated seasonal precipitation. The monsoonal flow pattern



81 and thus flow velocity is expected to be different than other rivers in the world, as a
82 consequence, k levels should be different than others, and potentially is higher in
83 subtropical monsoonal rivers.

84 Considerable efforts, such as purposeful (Jean-Baptiste and Poisson, 2000;
85 Crusius and Wanninkhof, 2003) and natural tracers (Wanninkhof, 1992) and FCs
86 (Borges *et al.*, 2004b; Guerin *et al.*, 2007; Alin *et al.*, 2011; Prytherch *et al.*, 2017),
87 have been carried out to estimate accurate k values. The direct determination of k by
88 FCs is more popular due to simplicity of the technique for short-term CO_2 flux
89 measurements (Raymond and Cole, 2001; Xiao *et al.*, 2014; Prytherch *et al.*, 2017).
90 Prior reports, however, have demonstrated that k values and the parameterization of k
91 as a function of wind and/or flow velocity (probably water depth) vary widely across
92 rivers and streams (Raymond and Cole, 2001; Raymond *et al.*, 2012). To contribute to
93 this debate, extensive investigation was accomplished for determination of k in rivers
94 and streams of the upper Yangtze using FC method. Our new contributions to the
95 literature are (1) providing first determination of k levels for small rivers and streams
96 in China, and (2) comparisons of two methods for CO_2 areal fluxes by FCs and
97 models developed. The outcome of this study is expected to help in accurate
98 estimation of CO_2 evasion from subtropical rivers and streams, and thus refine
99 riverine C budget over a regional/basin scale.

100

101 **2. Materials and methods**

102 **2.1. Study areas**



103 All field measurements were carried out in the rivers and streams of the Three
104 Gorges Reservoir (TGR) region (28°44′–31°40′N, 106°10′–111°10′E) that is locating
105 in the upper Yangtze River, China (Fig. S1). This region is subject to humid
106 subtropical monsoon climate with an average annual temperature ranging between 15
107 and 19 °C. Average annual precipitation is approx. 1250 mm with large intra- and
108 inter-annual variability. About 75% of the annual total rainfall is concentrated in April
109 through September.

110 The river sub-catchments include large scale river networks covering the
111 majority of the tributaries of the Yangtze in the TGR region, i.e., 32 first-order
112 tributaries and 16 second-order tributaries. These tributaries have drainage areas that
113 vary widely from 100 to 4400 km² with width ranging from 1 m to less than 100 m.
114 The annual discharges from these tributaries have a broad spectrum of 1.8 – 112 m³/s.
115 Detailed samplings were conducted in the two largest rivers of Daning (35 sampling
116 sites) and Qijiang (32 sites) in the TGR region. These two river basins drain
117 catchment areas of 4200 and 4400 km² with maximal third-order tributaries. The
118 location of sampling sites is deciphered in Fig. S1. The detailed information on
119 sampling sites and primary data are presented in the Supplement Materials (Appendix
120 Table A1). The sampling sites are outside the Reservoirs and are not affected by dam
121 operation.

122

123 2.2. Water sampling and analyses



124 Three fieldwork campaigns from the main river networks in the TGR region
125 were undertaken during May through August in 2016 (i.e., 18-22 May for Daning, 21
126 June-2 July for the entire tributaries of TGR, and 15-18 August for Qijiang). A total
127 of 115 discrete grab samples were collected (each sample consists of three replicates).
128 Running waters were taken using pre acid-washed 5-L high density polyethylene
129 (HDPE) plastic containers from depths of 10 cm below surface. The samples were
130 filtered through pre-baked Whatman GF/F (0.7- μm pore size) filters on the sampling
131 day and immediately stored in acid-washed HDPE bottles. The bottles were
132 transported in ice box to the laboratory and stored at 4 °C for analysis. Concentrations
133 of dissolved organic carbon (DOC), dissolved total nitrogen (DTN), and dissolved
134 total phosphorus (DTP) were determined within 7 days of water collection (Mao *et al.*,
135 2017).

136 Water temperature (T), pH, DO saturation (DO%) and electrical conductivity
137 (EC) were measured *in situ* by the calibrated multi-parameter sondes (HQ40d HACH,
138 USA, and YSI 6600, YSI incorporated, USA). pH, the key parameter for $p\text{CO}_2$
139 calculation, was measured to a precision of ± 0.002 , and pH sonde is calibrated by the
140 certified reference materials (CRMs) before measurements with an accuracy is better
141 than 0.2%. Atmospheric CO_2 concentrations were determined *in situ* using PP
142 Systems EGM-4 (USA). Total alkalinity was measured using a fixed endpoint
143 titration method with 0.0200 mol/L hydrochloric acid (HCl) on the sampling day.
144 DOC concentration was measured using a total organic carbon analyzer (TOC-5000,
145 Shimadzu, Japan) with a precision better than 3% (Mao *et al.*, 2017). DTN and DTP



146 concentrations were determined using a continuous-flow autoanalyzer (AA3, Seal
147 Analytical, Germany) and/or spectrophotometer following peroxodisulfate oxidation
148 (Ebina *et al.*, 1983). Analytical reagent grade chemical were used for all experiments.

149 Wind speed at 1 m over the water surface (U_1) and air temperature (T_a) were
150 measured with a Testo 410-1 handheld anemometer (Germany). Wind speed at 10 m
151 height (U_{10} , unit in m/s) was calculated using the following formula (Crusius and
152 Wanninkhof, 2003):

$$153 \quad U_{10} = U_Z \left[1 + \frac{(C_{d10})^{1/2}}{K} \times \ln\left(\frac{10}{z}\right) \right] \quad (3)$$

154 where C_{d10} is the drag coefficient at 10 m height (0.0013 m/s), and K is the von
155 Karman constant (0.41), and z is the height (m) of wind speed measurement. The
156 relationship was yielded when $z=1$ ($U_{10}=1.208 \times U_1$).

157 Aqueous $p\text{CO}_2$ was computed from the measurements of pH, total alkalinity, and
158 water temperature using CO_2 system (k_1 and k_2 are from Millero, 1979), which have
159 been identified as high quality data (Borges *et al.*, 2004a; Li *et al.*, 2012; Li *et al.*,
160 2013).

161

162 **2.3. Water-to-air CO_2 fluxes using FC method**

163 FCs (30 cm in diameter, 30 cm in height) were deployed to measure air-water
164 CO_2 fluxes and transfer velocities. They were made of cylindrical polyvinyl chloride
165 (PVC) pipe with a volume of 21.20 L and a surface area of 0.071 m^2 . These
166 non-transparent, thermally insulated vertical tubes, covered by aluminum foil, were



167 connected *via* CO₂ impermeable tubing (with outer and inner diameters of 0.5 cm and
168 0.35 cm, respectively) to a portable non-dispersive infrared CO₂ analyzer EGM-4
169 (PPSystems). Air was circulated through the EGM-4 instrument *via* an air filter using
170 an integral DC pump at a flow rate of 350 ml/min. The chamber method was widely
171 used and more details of advantages and limits on chambers were reviewed elsewhere
172 (Borges *et al.*, 2004b; Alin *et al.*, 2011; Xiao *et al.*, 2014).

173 Chamber measurements were conducted by deploying two replicate chambers or
174 one chamber for two times at each site. Data were logged automatically and
175 continuously at 1-min interval over a given span of time (normally 5-10 minutes) after
176 enclosure. The CO₂ area flux (mg/m²/h) was calculated using the following formula.

$$177 \quad F = 60 \times \frac{dp_{CO_2} \times M \times P \times T_0}{dt \times V_0 \times P_0 \times T} H \quad (4)$$

178 Where dp_{CO_2}/dt is the rate of concentration change in FCs ($\mu\text{l/l/min}$); M is the molar
179 mass of CO₂ (g/mol); P is the atmosphere pressure of the sampling site (Pa); T is the
180 chamber absolute temperature of the sampling time (K); V₀, P₀, T₀ is the molar
181 volume (22.4 l/mol), P₀ is atmosphere pressure (101325 Pa), and T₀ is absolute
182 temperature (273.15 K) under the standard condition; H is the chamber height above
183 the water surface (m) (Alin *et al.*, 2011). We accepted the flux data that had a good
184 linear regression of flux against time ($R^2 \geq 0.95$, $p < 0.01$).

185

186 **2.4. Calculations of the gas transfer velocity**

187 The k was computed with eq (1). To make comparisons, k is normalized to a Schmidt
188 (Sc) number of 600 (k_{600}) at a temperature of 20 °C.



189
$$k_{600} = k_T \left(\frac{600}{S_{CT}} \right)^{-0.5} \quad (5)$$

190
$$S_{CT} = 1911.1 - 118.11T + 3.4527T^2 - 0.04132T^3 \quad (5)$$

191 Where k_T is the measured values at the *in situ* temperature (T, unit in °C), S_{CT} is the
192 Schmidt number of temperature T. Dependency of k proportional to $Sc^{-0.5}$ was
193 employed here as measurement were made in highly turbulent rivers and streams in
194 this study (Wanninkhof, 1992; Borges *et al.*, 2004b; Alin *et al.*, 2011).

195

196 2.5. Data processing

197 Prior to statistical analysis, we excluded k_{600} data for samples with the air-water
198 pCO_2 gradient $< 110 \mu\text{atm}$, since the error in the k_{600} calculations drastically enhances
199 when ΔpCO_2 approaches zero (Borges *et al.*, 2004b). Spatial differences (Daning,
200 Qijiang and entire tributaries of TGR region) were tested using the nonparametric
201 Mann Whitney U-test. Multivariate statistics, such as correlation and stepwise
202 multiple linear regression, were performed for the models of k_{600} using potential
203 physical parameters, such as wind speed, water depth, and current velocity (Alin *et al.*,
204 2011). All statistical relationships were significant at $p < 0.05$. The statistical
205 processes were conducted using SigmaPlot 11.0 and SPSS 16.0 for Windows (Li *et al.*,
206 2009; Li *et al.*, 2016).

207

208 3. Results

209 3.1. CO_2 partial pressure and key water quality variables

210 The significant spatial variations in water temperature, pH, pCO_2 , DOC and



211 nutrients (DTN and DTP) were observed among Daning, TGR and Qijiang rivers
212 whereas alkalinity did not display such variability (Fig. S2). pH varied from 7.47 to
213 9.38 (mean of 8.39 ± 0.29) and lower pH was observed in TGR rivers (8.21 ± 0.33)
214 (Table 1; Fig. S2). pCO_2 varied between 50 and 4830 μatm with mean of 846 ± 819
215 μatm (Table 1), suggesting that all three rivers are supersaturated with reference to
216 atmospheric CO_2 and act as a source for the atmospheric CO_2 . The pCO_2 levels were
217 2.1 to 2.6-fold higher in TGR rivers than Daning ($483 \pm 294 \mu atm$) and Qijiang
218 Rivers ($614 \pm 316 \mu atm$) (Fig. S2). The calculated pCO_2 levels were within the
219 published range, but towards the lower-end of published concentrations compiled
220 elsewhere (Cole and Caraco, 2001; Li *et al.*, 2013). The total mean pCO_2 ($846 \mu atm$)
221 in the TGR, Daning and Qijiang sampled is lower than one third of global river's
222 average ($3220 \mu atm$) (Cole and Caraco, 2001).

223 The higher concentrations of dissolved organic carbon (DOC) and dissolved
224 nutrients (DTN and DTP) (Fig. S3) were observed in the TGR rivers than Qijiang and
225 Daning. Relatively higher concentrations of DOC and DTN were observed in Qijiang
226 than Daning River but mean TDP was much higher in latter than former river (Fig. S3;
227 Table 1).

228

229 3.2. CO_2 flux using floating chambers

230 The calculated CO_2 areal fluxes were higher in TGR rivers (217.7 ± 334.7
231 $mmol/m^2/d$, $n = 35$), followed by Daning ($122.0 \pm 239.4 mmol/m^2/d$, $n = 28$) and
232 Qijiang rivers ($50.3 \pm 177.2 mmol/m^2/d$, $n = 32$) (Fig. 1). The higher CO_2 evasion



233 from the TGR rivers is consistent with high riverine $p\text{CO}_2$ levels. The mean CO_2
234 emission rate was $133.1 \pm 269.1 \text{ mmol/m}^2/\text{d}$ ($n = 95$) in all three rivers sampled. The
235 mean CO_2 flux differed significantly between TGR rivers and Qijiang (Fig. 1). The
236 ratio of mean to median of CO_2 areal flux ranged between 1.4 (Qijiang) and 2.6 (TGR
237 rivers).

238

239 3.3. k levels

240 Samples with $\Delta p\text{CO}_2$ less than $110 \mu\text{atm}$ were excluded for k_{600} calculations, thus
241 a total of 64 data were used (10 for Daning River, 33 for TGR rivers and 21 for
242 Qijiang River) to develop k model (Table 2). No significant variability in k values
243 were observed among the three rivers sampled (Fig. 2). The mean k (unit in cm/h) is
244 relatively higher in Qijiang (60.2 ± 78.9), followed by Daning (50.2 ± 20.1) and TGR
245 rivers (40.4 ± 37.6), while the median k (unit in cm/h) was higher in Daning (50.5),
246 followed by TGR rivers (30.0) and Qijiang (25.8) (Fig. 2; Table S1). Binned k_{600} data
247 were averaged to $48.4 \pm 53.2 \text{ cm/h}$ (95% CI: 35.1-61.7), and it is 1.5-fold higher than
248 the median value (32.2 cm/h) (Fig. 2).

249

250 4. Discussion

251 We derived first-time the k values in the subtropical streams and small rivers.
252 Our measured k_{600} levels with a 95% CI of 35.1 to 61.7 (mean: 48.4) cm/h is
253 compared well with a compilation of data for streams and small rivers (e.g., 3-70
254 cm/h) (Raymond *et al.*, 2012). Our determined k values are greater than the global



255 rivers' average (8 - 33 cm/h) (Butman and Raymond, 2011; Raymond *et al.*, 2013),
256 and much higher than mean for tropical and temperate large rivers (5-31 cm/h) (Alin
257 *et al.*, 2011). These studies evidences that k_{600} values are highly variable in streams
258 and small rivers (Alin *et al.*, 2011; Ran *et al.*, 2015). Though the mean k in the TGR,
259 Daning and Qijiang is higher than global mean, however, it is consistent with k values
260 in the main stream and river networks of the turbulent Yellow River (42 ± 17 cm/h)
261 (Ran *et al.*, 2015), and Yangtze (38 ± 40 cm/h) (Liu *et al.*, 2017).

262 It has been well established that k is governed by a multitude of physical factors
263 particularly current velocity, wind speed, stream slope and water depth, of which,
264 wind speed is the dominant factor of k in open waters such as large rivers and
265 estuaries (Raymond and Cole, 2001; Crusius and Wanninkhof, 2003; Borges *et al.*,
266 2004b; Alin *et al.*, 2011). In contrast k in small rivers and streams is closely linked to
267 flow velocity, water depth and channel slope (Alin *et al.*, 2011; Raymond *et al.*, 2012).
268 Several studies reported that the combined contribution of flow velocity and wind
269 speed to k is significant in the large rivers (Beaulieu *et al.*, 2012; Ran *et al.*, 2015).
270 Thus, k values are higher in the Yellow River (ca. 0-120 cm/h) as compared to the
271 low-gradient River Mekong (0-60 cm/h) (Alin *et al.*, 2011; Ran *et al.*, 2015), due to
272 higher wind speed and flow velocity in the Yellow River (1.8 m/s) than Mekong river
273 (0.9 ± 0.4 m/s), resulting in greater surface turbulence and higher k level in the Yellow
274 (42 ± 17 cm/h) than Mekong river (15 ± 9 cm/h). The higher k values in the TGR,
275 Daning and Qijiang rivers are due to mountainous terrain catchment, high current
276 velocity (10 – 150 cm/s) (Fig. 3b), bottom roughness, and shallow water depth (10 -



277 150 cm) (Fig. 3a). It has been suggested that shallow water enhances bottom shear,
278 and the resultant turbulence increases k values (Alin *et al.*, 2011; Raymond *et al.*,
279 2012). These physical controls are highly variable across environmental types (Figs.
280 3a and 3b), hence, k values are expected to vary widely (Fig. 2). The k values in the
281 TGR rivers showed wider range (1-177 cm/h; Fig. 2; Table S1), spanning more than 2
282 orders of magnitude across the region, and it is consistent with the considerable
283 variability in the physical processes on water turbulence across environmental settings.
284 Similar broad range of k_{600} levels was also observed in the China's Yellow basin (ca.
285 0-123 cm/h) (Ran *et al.*, 2015; Ran *et al.*, 2017).

286 Contrary to our expectations, no significant relationship was observed between
287 k_{600} and water depth, and current velocity using the entire data in the TGR, Danning
288 and Qjiang rivers (Fig. S5). There were not statistically significant relationships
289 between k and wind speed and it is consistent with earlier studies (Alin *et al.*, 2011;
290 Raymond *et al.*, 2012). Flow velocity showed linear relation with k , and the extremely
291 high value of k was observed during the periods of higher flow velocity (Fig. S5a).
292 Similar trend was also observed between water depth and k values (Fig. S5b). The
293 lack of strong correlation between k and physical factors are probably due to
294 combined effect of both flow velocity and water depth, as well as large diversity of
295 channel morphology, both across and within river networks in the entire catchment
296 (60, 000 km²). This is further collaborated by weak correlations between k and flow
297 velocity in TGR rivers (Fig. 3), where one or two samples were taken for a large scale
298 examination. k_{600} as a function of water depth was obtained in TGR rivers, but it



299 explained only 30% of the variance in k_{600} . However, model using data from Qijiang
300 could explain 68% of the variance in k_{600} (Fig. 3b), and it was in line with general
301 theory. Nonetheless, k from our flow velocity based model (Fig. 3b) is largely
302 overestimated with consideration of other measurements (Alin *et al.*, 2015; Ran *et al.*,
303 2015; Ran *et al.*, 2017). When several extremely values are removed, k_{600} (cm/h) is
304 parameterized as follows ($k_{600} = 62.879FV + 6.8357$, $R^2 = 0.52$, $p = 0.019$, FV-flow
305 velocity with a unit of m/s), and this revised model is in good agreement with the
306 model in the river networks of the Yellow River (Ran *et al.*, 2017), but much lower
307 than the model developed in the Yangtze system (Liu *et al.*, 2017) (Fig. 3c). This is
308 reasonable because of k values in the Yangtze system are from large rivers with higher
309 turbulence than Yellow and our studied rivers. Furthermore, the measured k using FCs
310 was, on average, consistent with the revised model (Table 2).

311 The subtropical streams and small rivers are biologically more active and are
312 recognized to exert higher CO_2 areal flux to the atmosphere, however, their
313 contribution to riverine carbon cycling is still poorly quantified because of data
314 paucity and the absence of k in particular. Larger uncertainty of riverine CO_2 emission
315 in China was anticipated by use of k_{600} from other continents or climate zones. For
316 instance, k_{600} for CO_2 emission from tributaries in the Yellow River and karst rivers
317 was originated from the model in the Mekong (Zhang *et al.*, 2017), and Pearl (Yao *et*
318 *al.*, 2007), Longchuan (Li *et al.*, 2012), and Metropolitan rivers (Wang *et al.*, 2017),
319 which are mostly from temperate regions. Our k values will therefore largely improve
320 the estimation of CO_2 evasion from subtropical streams and small rivers, and improve



321 to refine riverine carbon budget. More studies, however, are clearly needed to build
322 the model, based on flow velocity and slope/water depth given the difficulty in k
323 quantification on a large scale.

324 We compared CO₂ areal flux by FCs and models developed here (Fig. 3) and
325 other studies (Alin *et al.*, 2011) (Tables 2 and 3). CO₂ evasion was estimated for rivers
326 in China with k values ranged between 8 and 15 cm/h (Yao *et al.*, 2007; Wang *et al.*,
327 2011; Li *et al.*, 2012) (Table S2). These estimates of CO₂ evasion rate were
328 considerably lower than using present k values (48.4±53.2 cm/h). For instance, CO₂
329 emission rates in the Longchuan River (e.g., k=8 cm/h) and Pearl River tributaries
330 (e.g., k=8-15 cm/h) were 3 to 6 times higher using present k values compared to
331 earlier. We found that the determined k average was marginally beyond the levels
332 from water depth based model and the model developed by Alin *et al.* (Alin *et al.*,
333 2011), while equivalent to the flow velocity based revised model, resulting in similar
334 patterns of CO₂ emission rates (Table 2). Hence selection of k values would
335 significantly hamper the accuracy of the flux estimation. Therefore k must be
336 estimated along with *p*CO₂ measurements to accurate flux estimations.

337 We used our measured CO₂ emission rates by FCs for upscaling flux estimates
338 and it was found to be 1.39 TgCO₂/y for all rivers sampled in our study (Table 3a).
339 The estimated emission was close to that of the revised model (1.40 ± 1.31 (95%
340 confidence interval: 0.91-1.87) Tg CO₂/y), and using the determined k average, i.e.,
341 1.37 ± 1.28 (95% confidence interval: 0.89-1.84) Tg CO₂/y, but slightly higher than
342 the estimation using water-depth based model (1.08 ± 1.01 Tg CO₂/y) and Alin's



343 model (1.06 ± 1.00 Tg CO₂/y) (Table 3b). The estimate was within the range of our
344 earlier work using TBL on the TGR river networks (0.64-2.33 Tg CO₂/y) (Li *et al.*,
345 2018). The higher emission, i.e., 3.29 ± 3.08 (2.15-4.43) Tg CO₂/y, using flow
346 velocity based model may be over-estimated (Table 3b). Therefore, this study
347 suggests that CO₂ emissions from rivers and streams in this area may be
348 underestimated, i.e., 0.03 Tg CO₂/y (Li *et al.*, 2017) and 0.37-0.44 Tg CO₂/y (Yang *et*
349 *al.*, 2013) as the former used TBL model with a lower k level, and the latter employed
350 floating chambers, but they both sampled very limited tributaries (i.e., 2-3 rivers).
351 Therefore, measurements of k must be made mandatory along with pCO₂
352 measurement in the river and stream studies.

353

354 5. Conclusion

355 We provided first determination of gas transfer velocity (k) in the subtropical
356 streams and small rivers. High variability in k values (mean 48.4 ± 53.2 cm/h) was
357 observed, reflecting the variability of morphological characteristics on water
358 turbulence both within and across river networks. The determined k using floating
359 chambers (FCs) was comparable to our newly water depth based model, while
360 substantially lower than flow velocity based model. We highlighted that k estimate
361 from empirical model should be pursued with caution and the significance of
362 incorporating k measurements along with extensive pCO₂ investigation is highly
363 essential for upscaling to watershed/regional scale carbon (C) budget.

364 Riverine pCO₂ and CO₂ areal flux showed pronounced spatial variability with



365 much higher levels in the TGR rivers. The CO₂ areal flux was averaged at 133.1 ±
366 269.1 mmol/m²/d using FCs, the resulting emission was around 1.39 Tg CO₂/y,
367 similar to the scaling up emission with the determined k, and the revised flow velocity
368 based model, while marginally above the water depth based model. More work is
369 clearly needed to refine the k modeling for evaluating regional C budgets.

370

371 **Acknowledgements**

372 This study was funded by “the Hundred-Talent Program” of the Chinese Academy of
373 Sciences (R53A362Z10; granted to Dr. Li), and the National Natural Science
374 Foundation of China (Grant No. 31670473). We are grateful to Mrs. Maofei Ni and
375 Tianyang Li, and Miss Jing Zhang for their assistance in the field works. Users can
376 access the original data from an Appendix.



377 References

- 378 Alin, S.R., Maria, D.F.F.L.R., Salimon, C.I., Richey, J.E., Holtgrieve, G.W., Krusche, A.V., Snidvongs, A.,
379 2015. Physical controls on carbon dioxide transfer velocity and flux in low - gradient river systems and
380 implications for regional carbon budgets. *Journal of Geophysical Research Biogeosciences* 116,
381 248-255.
- 382 Alin, S.R., Raseira, M., Salimon, C.I., Richey, J.E., Holtgrieve, G.W., Krusche, A.V., Snidvongs, A., 2011.
383 Physical controls on carbon dioxide transfer velocity and flux in low-gradient river systems and
384 implications for regional carbon budgets. *Journal of Geophysical Research-Biogeosciences* 116.
- 385 Bastviken, D., Tranvik, L.J., Downing, J.A., Crill, P.M., Enrich-Prast, A., 2011. Freshwater Methane
386 Emissions Offset the Continental Carbon Sink. *Science* 331, 50-50.
- 387 Beaulieu, J.J., Shuster, W.D., Rebholz, J.A., 2012. Controls on gas transfer velocities in a large river.
388 *Journal of Geophysical Research-Biogeosciences* 117.
- 389 Borges, A.V., Delille, B., Schiettecatte, L.S., Gazeau, F., Abril, G., Frankignoulle, M., 2004a. Gas transfer
390 velocities of CO₂ in three European estuaries (Randers Fjord, Scheldt, and Thames). *Limnology &*
391 *Oceanography* 49, 1630-1641.
- 392 Borges, A.V., Delille, B., Schiettecatte, L.S., Gazeau, F., Abril, G., Frankignoulle, M., 2004b. Gas transfer
393 velocities of CO₂ in three European estuaries (Randers Fjord, Scheldt, and Thames). *Limnology and*
394 *Oceanography* 49, 1630-1641.
- 395 Butman, D., Raymond, P.A., 2011. Significant efflux of carbon dioxide from streams and rivers in the
396 United States. *Nature Geoscience* 4, 839-842.
- 397 Cole, J.J., Caraco, N.F., 2001. Carbon in catchments: connecting terrestrial carbon losses with aquatic
398 metabolism. *Marine and Freshwater Research* 52, 101-110.
- 399 Cole, J.J., Prairie, Y.T., Caraco, N.F., McDowell, W.H., Tranvik, L.J., Striegl, R.G., Duarte, C.M., Kortelainen,
400 P., Downing, J.A., Middelburg, J.J., Melack, J., 2007. Plumbing the Global Carbon Cycle: Integrating
401 Inland Waters into the Terrestrial Carbon Budget. *Ecosystems* 10, 172-185.
- 402 Crusius, J., Wanninkhof, R., 2003. Gas transfer velocities measured at low wind speed over a lake.
403 *Limnology and Oceanography* 48, 1010-1017.
- 404 Ebina, J., Tsutsui, T., Shirai, T., 1983. SIMULTANEOUS DETERMINATION OF TOTAL NITROGEN AND TOTAL
405 PHOSPHORUS IN WATER USING PEROXODISULFATE OXIDATION. *Water Research* 17, 1721-1726.
- 406 Guerin, F., Abril, G., Serca, D., Delon, C., Richard, S., Delmas, R., Tremblay, A., Varfalvy, L., 2007. Gas
407 transfer velocities of CO₂ and CH₄ in a tropical reservoir and its river downstream. *Journal of Marine*
408 *Systems* 66, 161-172.
- 409 Jean-Baptiste, P., Poisson, A., 2000. Gas transfer experiment on a lake (Kerguelen Islands) using He-3
410 and SF₆. *Journal of Geophysical Research-Oceans* 105, 1177-1186.
- 411 Lauerwald, R., Laruelle, G.G., Hartmann, J., Ciais, P., Regnier, P.A.G., 2015. Spatial patterns in CO₂
412 evasion from the global river network. *Global Biogeochemical Cycles* 29, 534-554.
- 413 Li, S., Bush, R.T., 2015. Revision of methane and carbon dioxide emissions from inland waters in India.
414 *Global Change Biology* 21, 6-8.
- 415 Li, S., Bush, R.T., Ward, N.J., Sullivan, L.A., Dong, F., 2016. Air-water CO₂ outgassing in the Lower Lakes
416 (Alexandrina and Albert, Australia) following a millennium drought. *Science of the Total Environment*
417 542, 453-468.
- 418 Li, S., Gu, S., Tan, X., Zhang, Q., 2009. Water quality in the upper Han River basin, China: The impacts
419 of land use/land cover in riparian buffer zone. *Journal of Hazardous Materials* 165, 317-324.



- 420 Li, S., Ni, M., Mao, R., Bush, R.T., 2018. Riverine CO₂ supersaturation and outgassing in a subtropical
421 monsoonal mountainous area (Three Gorges Reservoir Region) of China. *Journal of Hydrology* 558,
422 460-469.
- 423 Li, S., Wang, F., Luo, W., Wang, Y., Deng, B., 2017. Carbon dioxide emissions from the Three Gorges
424 Reservoir, China. *Acta Geochimica* <https://doi.org/10.1007/s11631-017-0154-6>
- 425 Li, S.Y., Lu, X.X., Bush, R.T., 2013. CO₂ partial pressure and CO₂ emission in the Lower Mekong River.
426 *Journal of Hydrology* 504, 40-56.
- 427 Li, S.Y., Lu, X.X., He, M., Zhou, Y., Li, L., Ziegler, A.D., 2012. Daily CO₂ partial pressure and CO₂
428 outgassing in the upper Yangtze River basin: A case study of the Longchuan River, China. *Journal of*
429 *Hydrology* 466, 141-150.
- 430 Liu, S., Lu, X.X., Xia, X., Yang, X., Ran, L., 2017. Hydrological and geomorphological control on CO₂
431 outgassing from low-gradient large rivers: An example of the Yangtze River system. *Journal of*
432 *Hydrology* 550, 26-41.
- 433 Mao, R., Chen, H., Li, S., 2017. Phosphorus availability as a primary control of dissolved organic carbon
434 biodegradation in the tributaries of the Yangtze River in the Three Gorges Reservoir Region. *Science of*
435 *the Total Environment* 574, 1472-1476.
- 436 Prytherch, J., Brooks, I.M., Crill, P.M., Thornton, B.F., Salisbury, D.J., Tjernstrom, M., Anderson, L.G.,
437 Geibel, M.C., Humborg, C., 2017. Direct determination of the air-sea CO₂ gas transfer velocity in Arctic
438 sea ice regions. *Geophysical Research Letters* 44, 3770-3778.
- 439 Ran, L., Li, L., Tian, M., Yang, X., Yu, R., Zhao, J., Wang, L., Lu, X.X., 2017. Riverine CO₂ emissions in the
440 Wuding River catchment on the Loess Plateau: Environmental controls and dam impoundment impact.
441 *Journal of Geophysical Research-Biogeosciences* 122, 1439-1455.
- 442 Ran, L.S., Lu, X.X., Yang, H., Li, L.Y., Yu, R.H., Sun, H.G., Han, J.T., 2015. CO₂ outgassing from the Yellow
443 River network and its implications for riverine carbon cycle. *Journal of Geophysical*
444 *Research-Biogeosciences* 120, 1334-1347.
- 445 Raymond, P.A., Cole, J.J., 2001. Gas exchange in rivers and estuaries: Choosing a gas transfer velocity.
446 *Estuaries* 24, 312-317.
- 447 Raymond, P.A., Hartmann, J., Lauerwald, R., Sobek, S., McDonald, C., Hoover, M., Butman, D., Striegl,
448 R., Mayorga, E., Humborg, C., Kortelainen, P., Duerr, H., Meybeck, M., Ciais, P., Guth, P., 2013. Global
449 carbon dioxide emissions from inland waters. *Nature* 503, 355-359.
- 450 Raymond, P.A., Zappa, C.J., Butman, D., Bott, T.L., Potter, J., Mulholland, P., Laursen, A.E., Mcdowell,
451 W.H., Newbold, D., 2012. Scaling the gas transfer velocity and hydraulic geometry in streams and small
452 rivers. *Limnology & Oceanography Fluids & Environments* 2, 41-53.
- 453 Tranvik, L.J., Downing, J.A., Cotner, J.B., Loiselle, S.A., Striegl, R.G., Ballatore, T.J., Dillon, P., Finlay, K.,
454 Fortino, K., Knoll, L.B., 2009. Lakes and reservoirs as regulators of carbon cycling and climate.
455 *Limnology & Oceanography* 54, 2298-2314.
- 456 Wang, F., Wang, B., Liu, C.Q., Wang, Y., Guan, J., Liu, X., Yu, Y., 2011. Carbon dioxide emission from
457 surface water in cascade reservoirs–river system on the Maotiao River, southwest of China.
458 *Atmospheric Environment* 45, 3827-3834.
- 459 Wang, X.F., He, Y.X., Yuan, X.Z., Chen, H., Peng, C.H., Zhu, Q., Yue, J.S., Ren, H.Q., Deng, W., Liu, H.,
460 2017. pCO₂ and CO₂ fluxes of the metropolitan river network in relation to the urbanization of
461 Chongqing, China. *Journal of Geophysical Research-Biogeosciences* 122, 470-486.
- 462 Wanninkhof, R., 1992. RELATIONSHIP BETWEEN WIND-SPEED AND GAS-EXCHANGE OVER THE OCEAN.
463 *Journal of Geophysical Research-Oceans* 97, 7373-7382.



- 464 Wanninkhof, R., Asher, W.E., Ho, D.T., Sweeney, C., McGillis, W.R., 2009. Advances in Quantifying
465 Air-Sea Gas Exchange and Environmental Forcing. *Annual Review of Marine Science* 1, 213-244.
- 466 Xiao, S., Yang, H., Liu, D., Zhang, C., Lei, D., Wang, Y., Peng, F., Li, Y., Wang, C., Li, X., Wu, G., Liu, L., 2014.
467 Gas transfer velocities of methane and carbon dioxide in a subtropical shallow pond. *Tellus Series*
468 *B-Chemical and Physical Meteorology* 66.
- 469 Yang, L., Lu, F., Wang, X., Duan, X., Tong, L., Ouyang, Z., Li, H., 2013. Spatial and seasonal variability of
470 CO₂ flux at the air-water interface of the Three Gorges Reservoir. *Journal of Environmental Sciences*
471 25, 2229-2238.
- 472 Yao, G.R., Gao, Q.Z., Wang, Z.G., Huang, X.K., He, T., Zhang, Y.L., Jiao, S.L., Ding, J., 2007. Dynamics Of
473 CO₂ partial pressure and CO₂ outgassing in the lower reaches of the Xijiang River, a subtropical
474 monsoon river in China. *Science of the Total Environment* 376, 255-266.
- 475 Zhang, T., Li, J., Pu, J., Martin, J.B., Khadka, M.B., Wu, F., Li, L., Jiang, F., Huang, S., Yuan, D., 2017. River
476 sequesters atmospheric carbon and limits the CO₂ degassing in karst area, southwest China. *Science*
477 *of The Total Environment* 609, 92-101.
- 478



479 **Table 1.** Statistics of all the data from rivers.

	Water T (°C)	pH	Alkalinity (µeq/l)	pCO ₂ (µatm)	DO%	DOC (mg/L)	TDN (mg/L)	TDP (µg/L)	
Number	115	115	115	115	56	114	114	113	
Mean	22.5	8.39	2589.1	846.4	91.5	6.67	2.42	65.9	
Median	22.8	8.46	2560	588.4	88.8	2.51	1.56	50.7	
Std. Deviation	6.3	0.29	640.7	818.5	8.7	7.62	2.38	56.3	
Minimum	11.7	7.47	600	50.1	79.9	0.33	0.01	5.0	
Maximum	34	9.38	4488	4830.4	115.9	37.48	10.54	298.5	
Percentiles	25	16.3	8.24	2240	389.8	84.0	1.33	0.62	25.1
	75	29	8.56	2920	920.4	99.1	9.96	3.61	88.1
95% CI for Mean	Lower Bound	21.4	8.33	2470.8	695.2	89.1	5.26	1.98	55.4
	Upper Bound	23.7	8.44	2707.5	997.6	93.8	8.09	2.86	76.4

480

481 CI-Confidence Interval.



482 **Table 2.** Comparison of different model for CO₂ areal flux estimation (unit is
 483 mmol/m²/d for CO₂ areal flux and cm/h for k₆₀₀).

484

CO ₂ areal flux ^a	From FC	Flow velocity-based model (Fig. 3b)	Water depth-based model (Fig.3a)	Alin's model	
k ₆₀₀	48.4 ^b	116.5 ^c	38.3	37.6	
Mean	198.1	476.7	156.6	154.0	
S.D.	185.5	446.2	146.6	144.2	
95% CI for Mean	Lower Bound	129.5	311.5	102.3	100.6
	Upper Bound	266.8	641.8	210.8	207.4

485

486 CI-Confidence Interval

487 a-CO₂ areal flux is based on TBL model.

488 b-mean level that is determined using floating chambers (FC).

489 c-This figure is revised to be 49.6 cm/h if the model ($k_{600} = 62.879FV + 6.8357$, $R^2 =$
 490 0.52 , $p=0.019$) is used (Fig. 3c), and the corresponding CO₂ areal flux is 203 ± 190
 491 mmol/m²/d.

492



493 **Table 3.** CO₂ emission from total rivers sampled in the study.

494 (a) Upscaling using CO₂ areal flux by FC.

	Catchment Area km ²	Water surface km ²	CO ₂ areal flux mmol/m ² /d	CO ₂ emission Tg CO ₂ /y
Danang	4200	21.42	122.0 ± 239.4	0.042
Qijiang	4400	30.8	50.3 ± 177.2	0.025
TGR river	50000	377.78	217.7 ± 334.7	1.321
Total				1.39

495

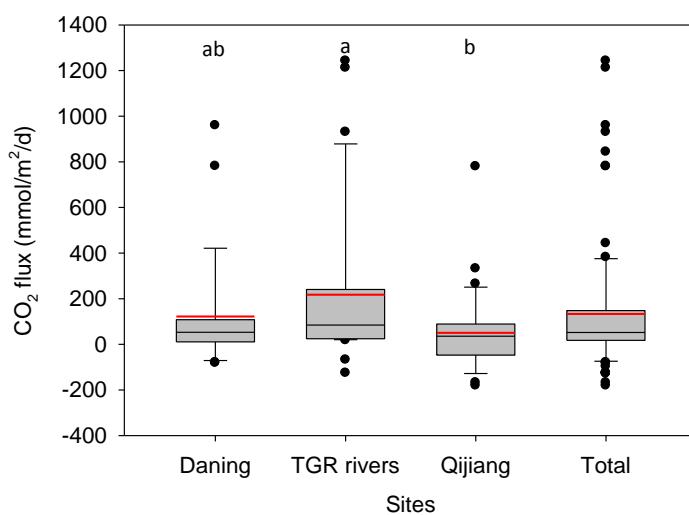
496 (b) Upscaling using determined k average and models (whole dataset are used here).

	From determined k mean	Flow velocity-based model (Fig. 3b) (numbers in bracket is from the revised model; Fig. 3c)	Water depth-based model (Fig. 3a)	Alin's model
Mean	1.37	3.29 (1.40)	1.08	1.06
S.D.	1.28	3.08 (1.31)	1.01	1.00
95% CI for Mean	Lower Bound 0.89	2.15 (0.91)	0.71	0.69
	Upper Bound 1.84	4.43 (1.81)	1.46	1.43

497 A total water area of approx. 430 km² for all tributaries (water area is from Landsat

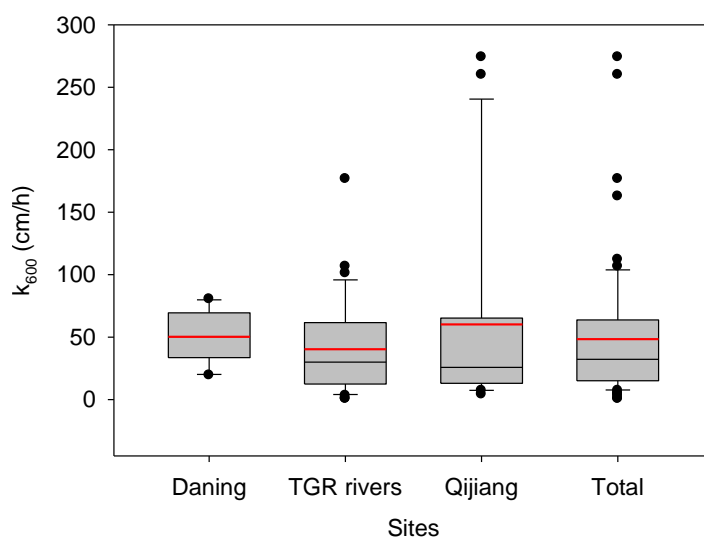
498 ETM+ in 2015).

499



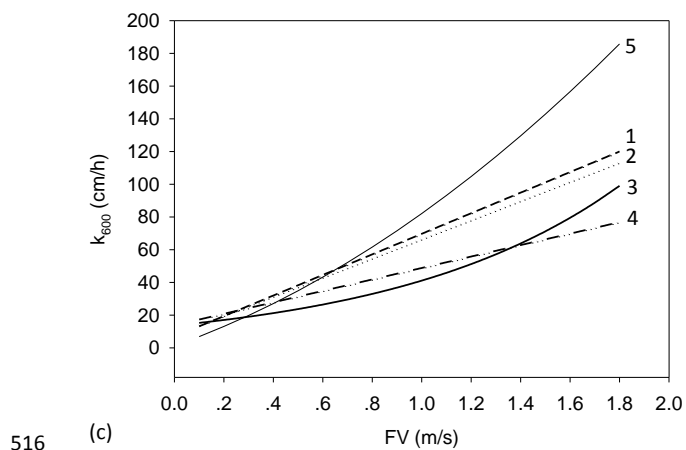
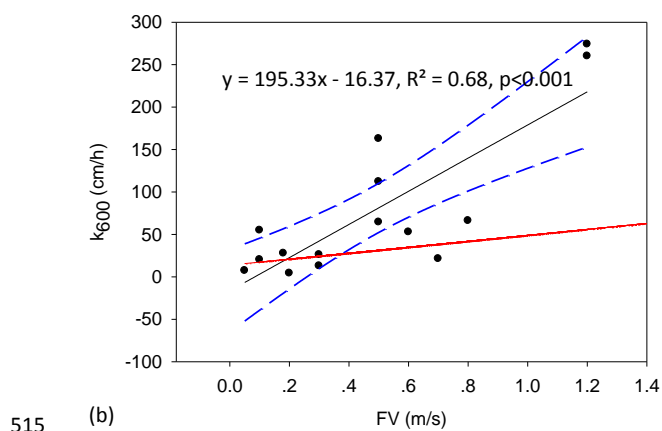
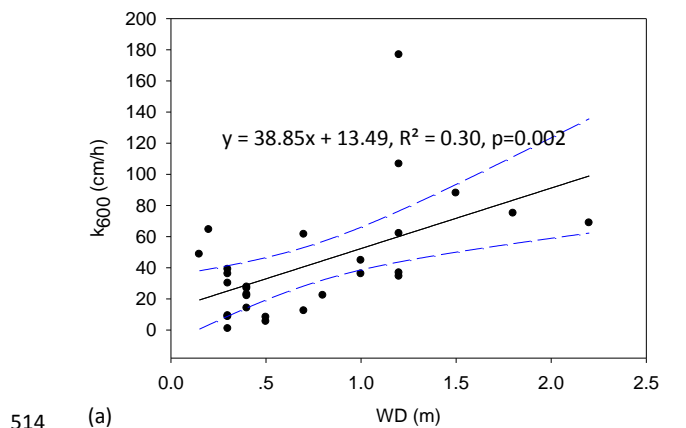
500

501 **Fig. 1.** Boxplots of CO₂ emission rates by floating chambers in the subtropical rivers
502 (different letters represent statistical differences at $p < 0.05$ by **Mann-Whitney Rank Sum**
503 **Test**). (the black and red lines, lower and upper edges, bars and dots in or outside the
504 boxes demonstrate median and mean values, 25th and 75th, 5th and 95th, and <5th
505 and >95th percentiles of all data, respectively). (For interpretation of the references
506 to color in this figure legend, the reader is referred to the web version of this article).



507

508 **Fig. 2.** Boxplots of k_{600} levels in the subtropical rivers (there is not a statistically
 509 significant difference in k among sites by Mann-Whitney Rank Sum Test). (the black
 510 and red lines, lower and upper edges, bars and dots in or outside the boxes
 511 demonstrate median and mean values, 25th and 75th, 5th and 95th, and <5th
 512 and >95th percentiles of all data, respectively). (For interpretation of the references
 513 to color in this figure legend, the reader is referred to the web version of this article).



518 **Fig. 3.** The k_{600} as a function of water depth (WD) in TGR rivers (a), flow velocity (FV)



519 in Qijiang (b), and comparison of the developed model with other models (c) (others
520 without significant relationships between k and physical factors are not shown). The
521 solid lines show regression, the dashed lines represent 95% confidence band, and the
522 red dash-dotted line represents the model developed by Alin et al (2011) (in panel b,
523 if several extremely values are removed, the revised model would be $k_{600} = 62.879FV$
524 $+ 6.8357$, $R^2 = 0.52$, $p=0.019$) (in panel c, 1-the revised model, 2-model from Ran et
525 al., 2017, 3-model from Ran et al., 2015, 4-model from Alin et al., 2011, 5-model
526 from Liu et al., 2017) (1- $k_{600} = 62.879FV + 6.8357$; 2- $k_{600} = 58.47FV+7.99$; 3- $k_{600} =$
527 $13.677\exp(1.1FV)$; 4- $k_{600} = 35 FV + 13.82$; 5- $k_{600} = 6.5FV^2 + 12.9FV+0.3$) (unit of k in
528 models 1-4 is cm/h, and unit of m/d for model 5 is transferred to cm/h).

529